

C-Sphere Strength-Size Scaling in a Bearing-Grade Silicon Nitride¹

Andrew A. Wereszczak^{*†}, Timothy P. Kirkland^{*}, Osama M. Jadaan^{**},
Kevin T. Strong^{*}, and Gregory J. Champoux^{*}

^{*}Ceramic Science and Technology Oak Ridge National Laboratory Oak Ridge, TN 37831, USA

^{**}College of Engineering, Mathematics, and Science University of Wisconsin -Platteville Platteville, WI 53818, USA

(Received June 8, 2008; Accepted August 31, 2008)

ABSTRACT

A “C-sphere” specimen geometry was used to determine the failure strength distributions of a commercially-available bearing-grade silicon nitride (Si_3N_4) with ball diameters of 12.7 and 25.4 mm. Strengths for both diameters were determined using the combination of failure load, C-sphere geometry, and finite element analysis and fitted using two-parameter Weibull distributions. Effective areas of both diameters were estimated as a function of Weibull modulus and used to explore whether the strength distributions predictably scaled between each size. They did not. That statistical observation suggested that the same flaw type did not limit the strength of both ball diameters indicating a lack of material homogeneity between the two sizes. Optical fractography confirmed that. It showed there were two distinct strength-limiting flaw types common to both ball diameters, that one flaw type was always associated with lower strength specimens, and that a significantly higher fraction of the 25.4-mm-diameter C-sphere specimens failed from it. Predictable strength-size-scaling would therefore not result as a consequence of this because these flaw types were not homogeneously distributed and sampled in both C-sphere geometries.

Key words : Silicon nitride, Bearing, C-sphere strength, Size scaling

1. Introduction

Silicon nitride (Si_3N_4) balls for use in hybrid bearings extend rolling contact fatigue (RCF) lifetime, reduce the dynamic loading in high-speed roller element applications because of their lower density compared to steel balls, and enable bearing use in more corrosive and higher temperature environments.¹⁻³⁾ During their development, many parameters such as density, hardness, elastic modulus, fracture toughness, 3- and 4-pt flexure strength and Weibull modulus, crushing strength, grain size and secondary phase morphology, porosity, and surface finish have been extensively studied in an effort to improve or predict RCF performance of Si_3N_4 balls.¹⁻⁷⁾ An ASTM standard on ceramic balls was developed as a consequence of much of that work.⁸⁾

However, because little study had been devoted to the quantification of surface and sub-surface flaws on actual finished balls, a “C-sphere” specimen geometry was developed to measure failure stress of actual bearing-grade silicon nitride (Si_3N_4) balls. Fracture is caused by tension at the ball’s surface⁹⁾ and it occurs at a modestly applied force. Surface-located strength-limiting flaws in ceramic spheres can then be readily studied with this specimen. Lastly, the uncertainty of whether or not some other specimen geometry (e.g., bend bars) is capturing the same flaw population

that exists in the sphere geometry is circumvented.

The geometry of the c-sphere is described in detail elsewhere⁹⁾ but is briefly described here. A slot is machined into the balls to a set depth. A monotonically increasing uniaxial compressive force applied diametrically produces an increasing tensile stress at the C-sphere’s outer surface that ultimately initiates fracture. The test method’s simplicity and versatility are illustrated by its use with spheres as small as 1-mm diameter.¹⁰⁾ The strength is determined using the combination of failure load, C-sphere geometry, and finite element analysis.

Though several different size balls have been characterized using the C-sphere test geometry with different Si_3N_4 grades, the authors wanted to examine if the established Weibull strength-size-scaling method for ceramics would represent strengths of different size balls made from the same Si_3N_4 . This study examines that using 12.7 and 25.4 mm diameter balls.

2. Experimental Procedures

The bearing-grade Si_3N_4 material tested was SN101C (Saint-Gobain, East Granby, CT). Much of its characterization conducted by the authors can be found in Refs. 2 and

[†]Corresponding author : Andrew A. Wereszczak
E-mail : wereszczakaa@ornl.gov
Tel : +1-865-576-1169 Fax : +1-865-574-6098

¹Research sponsored by the U.S. Department of Energy, Assistant Secretary for Energy Efficiency and Renewable Energy, Office of Vehicle Technologies, as part of the Propulsion Materials Program, under contract DE-AC05-00OR22725 with UT-Battelle, LLC.

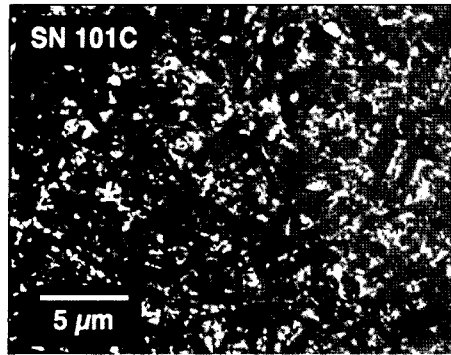


Fig. 1. Polished microstructure of SN101C Si_3N_4 .

Table 1. Definition of C-Sphere Geometrical Parameters Shown in Fig. 2

Label	Parameter	12.7 mm diameter	25.4 mm diameter
A	Diameter	12.7 mm	25.4 mm
B	Ligament Thickness	2.54 mm	5.08 mm
C	Slot Width	6.35 mm	12.7 mm
D	Offset	0.635 mm	1.27 mm
E	Slot Radius	3.175 mm	6.35 mm

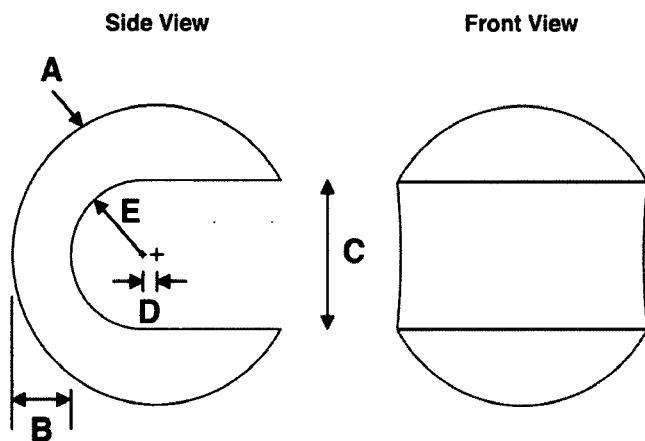


Fig. 2. Side and front views of the C-sphere flexure strength specimen. Shown symbols correspond to values in Table 1 for the two examined diameters.

11. Its microstructure is shown in Fig. 1. The elastic modulus and Poisson's ratio were measured to be 307 GPa and 0.27, respectively.¹¹⁾ While it exhibits an indentation size effect, its Vickers hardness is relatively constant between 10 and 100 N is approximately 14.7 GPa.¹¹⁾

A generic schematic of the C-sphere specimen is shown in Fig. 2. The machined dimensions used with the 12.7 and 25.4 mm diameter balls are listed in Table 1. They were produced by a commercial machine shop (Bomas, Somerville, MA) using the machining method presented in Ref. 9. Examples of the C-spheres for both diameters are shown in Fig. 3.

An electromechanical universal testing machine was used to monotonically load the samples in compression until fail-



Fig. 3. 12.7 mm diameter (left) and 25.4 mm diameter (right) C-spheres.

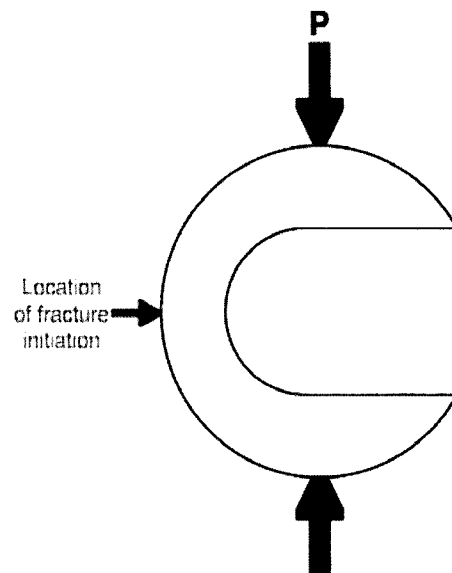


Fig. 4. Diametral compression of the C-sphere flexure specimen causes fracture initiation from a hoop stress at the outer fiber.

ure occurred. A schematic of the specimen's diametral loading is shown in Fig. 4. A special alignment jig was used to horizontally align the C-sphere slot prior to loading. A slight compressive preload (~ 25 N) was applied to the jugged C-sphere specimen enabling the jig to be pulled out without disturbing the C-sphere alignment. The specimens were then tested at a crosshead displacement rate of 0.5 mm/min. Load to fracture was recorded and used to determine C-sphere flexure strength. Compressive force is linear with maximum tensile stress for the c-sphere. For the dimensions listed in Table 1, each 100 N of compressive force produces a tensile stress of 66 MPa for both diameters. At least twenty-five C-sphere specimens of both diameters were tested. Weibull strength distributions were determined using commercially available software (WeibPar, Connecticut Reserve Technologies, Cleveland, OH).

The effective areas for the two C-sphere specimen geometries were determined as function of Weibull modulus using the CARES/Life(Connecticut Reserve Technologies, Cleveland, OH) software. As described in Ref. 9, particular attention was paid to the effect of mesh sensitivity and localized stress concentration under the applied point load on the

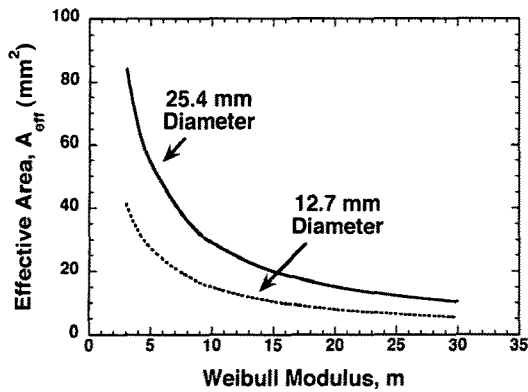


Fig. 5. Comparison of effective area as function of Weibull modulus for the two C-sphere diameters.

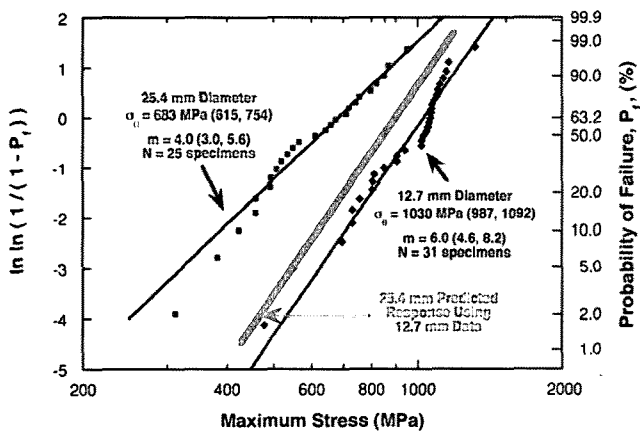


Fig. 6. Uncensored strength distributions for the two examined C-sphere diameters. Using the data from the 12.7-mm-diameter tests, the predicted strength distribution for the 25.4 mm did not correlate to the measured strength response.

effective sizes. These results enable the study of the predictability of strength-size-scaling. If the strengths of both C-sphere sets are limited by the same flaw type, then the strength prediction of one using the other's strength distribution will work.

3. Results and Discussion

The resulting effective areas for both diameters are shown

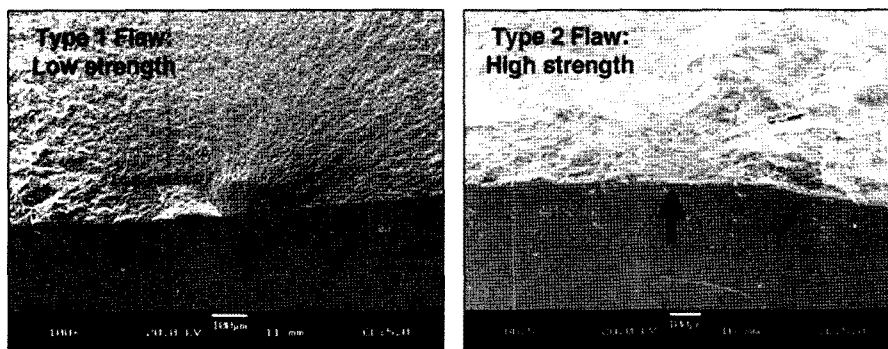


Fig. 7. Two flaw types were common to both C-sphere sizes. However, Type 1 always produced lower strengths and caused many more failures (16 of 25) in the 25.4 mm C-sphere than in the 12.7 mm C-sphere (2 of 31).

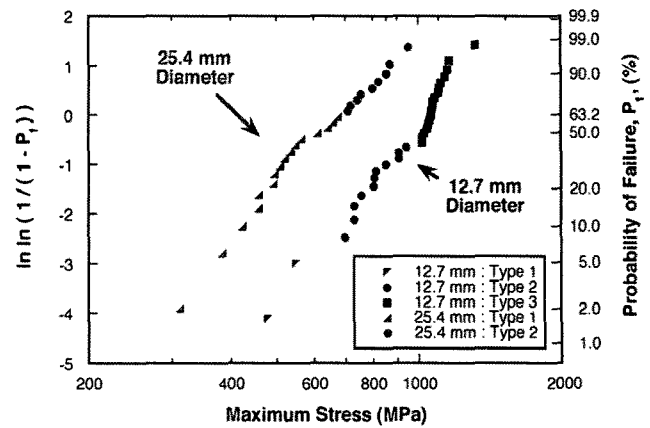


Fig. 8. Flaw type and respective distributions for both the 12.7 and 25.4 mm diameter C-sphere sets. The 12.7 mm and the 25.4 mm C-spheres had two of the same flaw types while the 12.7 C-spheres had a third flaw type not observed in the 25.4 mm c-spheres.

in Fig. 5. For a given Weibull modulus, the numerically estimated effective area for the 25.4 mm diameter C-sphere is almost exactly twice that for the 12.7 mm diameter C-sphere.

The measured uncensored strength distributions are illustrated in Fig. 6 and show the expected trend that the smaller diameter C-sphere was stronger. However, does established strength-size-scaling predict this difference? For such area-based scaling between any component A and B,

$$S_B = \left(\frac{K_{A,A} \cdot A_A}{K_{A,B} \cdot A_B} \right)^{1/m} S_A \quad (1)$$

where $K_{A,A}A_A$ and $K_{A,B}A_B$ are the effective areas for components A and B, A_A and A_B are the area of each component under tensile stress, K_A and K_B are the loading factors for A and B, S_A and S_B are the stress for A and B under the same probability of survival, and m is the Weibull modulus. Such established analysis implicitly assumes that the same strength-limiting flaw is controlling the failure of both components A and B (as represented by a single m value). Using an average Weibull modulus of 5 and the associated effective areas for both C-sphere sizes shown in Fig. 5 in Eq. 1, the characteristic strength of the 25.4 mm C-sphere should

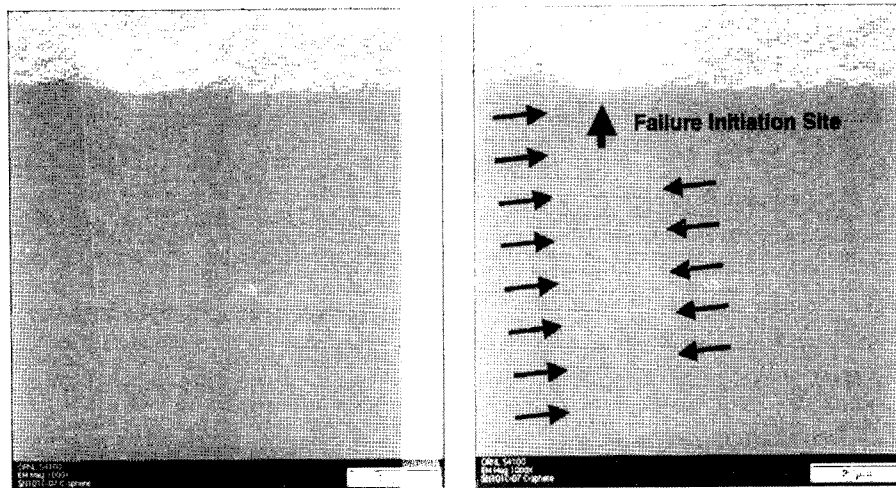


Fig. 9. Strength-limiting flaw type aligned with markings on finished surface.

be about 87% that of the 12.7 mm C-sphere. *The strengths of the 25.4 mm C-sphere are indeed much less than that, so given that this scaling is not an accurate predictor suggests that the strength-limiting flaw is not the same in both sets.*

Fractography showed that indeed there were two distinct strength-limiting flaw types found common to both C-sphere diameters. There was also a third flaw type observed in the 12.7 mm C-sphere set but not in the 25.4 mm set. The two flaw types common to both C-sphere sets are illustrated in Fig. 7. The weakest specimens of both sets were limited by Flaw Type 1; however, only two of the thirty-one 12.7 mm C-spheres were affected by that flaw type while a majority (sixteen of twenty-five) of the 25.4 mm diameter specimens were (see Fig. 8). The microstructure in and around Flaw Type 1 is shown in Figs. 9 and 10. It appears that these are surface-located microstructural regions containing a higher glassy content, and that their effect is more

pronounced in the 25.4 mm C-sphere. It is not known yet if this flaw type is distributed around the whole sphere's surface; obviously, the effective area of the C-ring only samples a fraction of the overall sphere's area, but given that the majority of the 25.4 mm C-spheres failed from it indicates they are likely quite prevalent on the original 25.4 mm sphere surface.

Predictable strength-size-scaling would not result as a consequence because these flaw types were not homogeneously distributed and sampled in both c-sphere geometries. This demonstrates the utility of the C-sphere test geometry for strength testing; it enabled fractography and the identification of discrete flaw types. Lastly, this study also demonstrates that strength-size-scaling needs to be done in concert with fractography and strength-data-censoring.

4. Conclusions

A "C-sphere" specimen geometry was used to diagnose strength and material state differences between 12.7 and 25.4 mm diameter balls of the same bearing-grade Si_3N_4 . An inability to strength-size-scale them was an indicator of those differences, and fractography showed that the 25.4 mm diameter balls were more apt to fail at low stresses from a flaw that was comprised of a surface-located microstructural region containing a higher concentration of a glassy phase. Promoting the activity of the same dominant strength-limiting flaw (i.e., material homogeneity) in both of these diameters should produce predictable strength-size-scaling.

Acknowledgments

The authors thank ORNL's H. -T. Lin and S. B. Waters for their assistance with the scanning electron microscopy, ORNL's W. L. Daloz for his assistance with some of the optical imaging, ORNL's M. Lance and A. Shyam for their review of this manuscript, and Alfred University's J. Var-



Fig. 10. Flaw type 1 was linked to a surface-located microstructure that had a glassy-like appearance.

ner for his fractographical guidance.

REFERENCES

1. L. -Y. Chao, D. K. Shetty, J. H. Adair, and J. J. Mecholsky, Jr., "Development of Silicon Nitride For Rolling-Contact Bearing Applications: A Review," *J. Mater. Educ.*, **17** 245-303 (1995).
2. L. Wang, R. W. Snidle, and L. Gu, "Rolling Contact Silicon Nitride Bearing Technology: A Review of Recent Research," *Wear*, **246** 159-73 (2000).
3. Y. Wang and M. Hadfield, "Rolling Contact Fatigue of Ceramics," Vol. 11, Section 6E, ASM Handbook, 2002.
4. H. I. Burrier, Jr., "Optimizing the Structure and Properties of Silicon Nitride for Rolling Contact Bearing Performance," *Tribol. Trans.*, **39** 276-85 (1996).
5. J. Kang, M. Hadfield, and R. T. Cundill, "Rolling Contact Fatigue Performance of HIPed Si_3N_4 with Different Surface Roughness," *Ceram. Int.*, **27** 781-94 (2001).
6. M. Ichikawa, T. Takamatsu, T. Matsuo, N. Okabe, and Y. Abe, "Ring Crack Initiation Load of Silicon Nitride Bearing Balls," *JSME Int. J. A: Mech. Mat. Eng.*, **38** 226-30 (1995).
7. R. T. Cundill, "Impact Resistance of Silicon Nitride Balls," pp. 556-61 in *Proc. 6th Int. Symp. Ceram. Mat. & Comp. Engines*, (1997).
8. "Standard Specification for Silicon Nitride Bearing Balls," ASTM F 2094-03a, Vol. 01.08, ASTM International, West Conshohocken, PA, 2004.
9. A. A. Wereszczak, T. P. Kirkland, and O. M. Jadaan, "Strength Measurement of Ceramic Spheres Using a Diametrically Compressed 'C-Sphere' Specimen," *J. Am. Ceram. Soc.*, **90** 1843-49 (2007).
10. A. A. Wereszczak, O. M. Jadaan, H. -T. Lin, G. J. Champoux, and D. P. Ryan, "Hoop Tensile Strength Testing of Small Diameter Ceramic Particles," *J. Nuc. Mats.*, **361** 121-25 (2007).
11. H. Wang and A. A. Wereszczak, "Mechanical Responses of Silicon Nitrides Under Dynamic Indentation," *Cer. Eng. Sci. Proc.*, **26** 275-83 (2005).